AFRL-RQ-WP-TR-2021-0056

ATOMIC LAYER DEPOSITION OF LITHIUM TANTALUM OXIDE SOLID-STATE ELECTROLYTE DEPOSITED OVER ZIRCONIUM OXIDE PROTECTED LITHIUM DISCS

Bo Yin and Jeffrey R. Alston
Joint School of Nanoscience and Nanoengineering
North Carolina Agricultural and Technical State University

JANUARY 2021
Final Report

AIR FORCE RESEARCH LABORATORY
AEROSPACE SYSTEMS DIRECTORATE
WRIGHT-PATTERSON AIR FORCE BASE, OH 45433-7542
AIR FORCE MATERIEL COMMAND
UNITED STATES AIR FORCE

NOTICE PAGE

Using Government drawings, specifications, or other data included in this document for any purpose other than Government procurement does not in any way obligate the U.S. Government. The fact that the Government formulated or supplied the drawings, specifications, or other data does not license the holder or any other person or corporation; or convey any rights or permission to manufacture, use, or sell any patented invention that may relate to them.

This paper was cleared for public release by the Air Force Research Laboratory Public Affairs Office (AFRL/PA) and is available to the general public, including foreign nationals.

Copies may be obtained from the Defense Technical Information Center (DTIC) (https://discover.dtic.mil).

AFRL-RQ-WP-TR-2021-0056 has been reviewed and is approved for publication in accordance with assigned distribution statement.

This paper is published in the interest of scientific and technical information exchange and its publication does not constitute the Government's approval or disapproval of its ideas or findings.

REPORT DOCUMENTATION PAGE

Form Approved
OMB No. 0704-0188

1. REPORT DATE *(DD-MM-YY)*	2. REPORT TYPE	3. DATES COVERED *(From - To)*
January 2021	Final	13 October 2017 – 31 December 2020

4. TITLE AND SUBTITLE
ATOMIC LAYER DEPOSITION OF LITHIUM TANTALUM OXIDE SOLID-STATE ELECTROLYTE DEPOSITED OVER ZIRCONIUM OXIDE PROTECTED LITHIUM DISCS

5a. CONTRACT NUMBER
FA8650-17-2-2228

5b. GRANT NUMBER

5c. PROGRAM ELEMENT NUMBER
62201F

6. AUTHOR(S)
Bo Yin and Jeffrey R. Alston

5d. PROJECT NUMBER
6206WF

5e. TASK NUMBER

5f. WORK UNIT NUMBER
Q01F

7. PERFORMING ORGANIZATION NAME(S) AND ADDRESS(ES)
Department of Nanoengineering
North Carolina Agricultural and Technical State University
1601 E Market St
Greensboro, NC 27411

8. PERFORMING ORGANIZATION REPORT NUMBER

9. SPONSORING/MONITORING AGENCY NAME(S) AND ADDRESS(ES)
Air Force Research Laboratory
Aerospace Systems Directorate
Wright-Patterson Air Force Base, OH 45433-7542
Air Force Materiel Command
United States Air Force

10. SPONSORING/MONITORING AGENCY ACRONYM(S)
AFRL/RQQE

11. SPONSORING/MONITORING AGENCY REPORT NUMBER(S)
AFRL-RQ-WP-TR-2021-0056

12. DISTRIBUTION/AVAILABILITY STATEMENT
DISTRIBUTION STATEMENT A. Approved for public release. Distribution is unlimited.

13. SUPPLEMENTARY NOTES
PA Clearance Number: AFRL-2021-2671; Clearance Date: 13 Aug 2021

14. ABSTRACT

We report the successful deposition of a lithium-tantalum oxide (LixTayOz) solid-state electrolyte on ZrO2-coated lithium discs using Plasma Enhanced Atomic Layer Deposition (PEALD). ZrO2 layers deposited on lithium discs successfully increased the lithium substrate's thermal stability, allowing the deposition temperature of the lithium tantalum oxide layer to be increased to 175 °C. A pulsing sequence of 1 × Li2O + 6 × Ta2O5 was used for the deposition process. The effects of different tantalum ethoxide (TaEO) pulse durations on the deposited lithium tantalum oxide film were also studied. The deposited solid-state electrolyte layer was characterized using SEM, XPS, AFM , and four-point probe conductivity. From this characterization, we confirmed the successful uniform deposition of a lithium tantalum oxide solid-state electrolyte. The deposition rate of the solid-state electrolyte averaged 6.3 Å per cycle as measured by AFM. The resistivity of the lithium tantalum film was 2.0 kΩ per square, which indicates that the solid-state electrolyte is electronically insulating and could help prevent energy leakage and side reactions in the battery. We observed two types of chemical binding energy within the lithium tantalum film: Li-O-Ta and Ta-O-Ta. The ratio of the two binding types is closely related to the TaEO pulse duration and the number of Ta2O5 subcycles. The composition of lithium tantalum oxide film, LixTayOz, can also be tuned by the number of Ta2O5 subcycles. We also found that Ta2O5 can prevent Li2O on the surface of the lithium tantalum oxide electrolyte layer from reacting with ambient CO2. Therefore, Ta2O5 can be used to increase the stability of the lithium tantalum oxide film. However, excess Ta in the lithium tantalum oxide film will reduce the Li+ conductivity of the deposited layer, which is detrimental to solid-state electrolyte applications.

15. SUBJECT TERMS
plasma enhanced atomic layer deposition, Li-ion battery

16. SECURITY CLASSIFICATION OF:			17. LIMITATION OF ABSTRACT:	18. NUMBER OF PAGES	19a. NAME OF RESPONSIBLE PERSON (Monitor)
a. REPORT	b. ABSTRACT	c. THIS PAGE			Alireza Behbahani
Unclassified	Unclassified	Unclassified	SAR	22	19b. TELEPHONE NUMBER (Include Area Code) N/A

TABLE OF CONTENTS

LIST OF FIGURES

LIST OF TABLES

1. SUMMARY

The successful deposition of a lithium-tantalum oxide ($Li_xTa_yO_z$) solid-state electrolyte on ZrO_2-coated lithium discs using Plasma Enhanced Atomic Layer Deposition (PEALD) in reported. ZrO_2 layers deposited on lithium discs successfully increased the lithium substrate's thermal stability, allowing the deposition temperature of the lithium tantalum oxide layer to be increased to 175 ℃. A pulsing sequence of 1 × Li_2O + 6 × Ta_2O_5 was used for the deposition process. The effects of different tantalum ethoxide (TaEO) pulse durations on the deposited lithium tantalum oxide film were also studied. The deposited solid-state electrolyte layer was characterized using scanning electron microscopy (SEM), x-ray photoelectron spectroscopy (XPS), atomic force microscopy (AFM), and four-point probe conductivity. From this characterization, we confirmed the successful uniform deposition of a lithium tantalum oxide solid-state electrolyte. The deposition rate of the solid-state electrolyte averaged 6.3 Å per cycle as measured by AFM. The resistivity of the lithium tantalum film was 2.0 kΩ per square, which indicates that the solid-state electrolyte is electronically insulating and could help prevent energy leakage and side reactions in the battery. We observed two types of chemical binding energy within the lithium tantalum film: Li-O-Ta and Ta-O-Ta. The ratio of the two binding types is closely related to the TaEO pulse duration and the number of Ta_2O_5 subcycles. The composition of lithium tantalum oxide film, $Li_xTa_yO_z$, can also be tuned by the number of Ta_2O_5 subcycles. We also found that Ta_2O_5 can prevent Li_2O on the surface of the lithium tantalum oxide electrolyte layer from reacting with ambient CO_2. Therefore, Ta_2O_5 can be used to increase the stability of the lithium tantalum oxide film. However, excess Ta in the lithium tantalum oxide film will reduce the Li+ conductivity of the deposited layer, which is detrimental to solid-state electrolyte applications.

More study is needed to optimize the deposition parameters of solid-state electrolytes.

2. INTRODUCTION

Electronic devices—such as phones, computers, and medical equipment—are essential to everyday life. The lithium-ion battery is the preferred energy source for charging these devices because of its ability to deliver high energy density. As technology advances, a next generation of lithium battery is needed. Among potential candidates, the solid-state state electrolyte lithium-ion battery has attracted a lot of attention from researchers around the world: it allows greater flexibility in battery design, improves user safety due to the absence of liquid electrolytes, and can further reduce battery size for application in microelectronic devices.[1-3] Currently, most research on lithium batteries concerns two-dimensional (2D) thin film. However, to further increase the capacity of lithium battery, a three-dimensional (3D) anode is needed. Solid-state electrolytes are especially suitable for a 3D anode with complicated architecture because, unlike liquid electrolytes, there is no solid-liquid phase separation. Therefore, 3D architecture can be used effectively as an anode in lithium batteries.

The key component in all solid-state batteries is a solid-state electrolyte which needs to have high ionic conductivity, low electronic conductivity, a high electrochemically stable voltage window, and be chemically and mechanically stable with electrodes. Atomic layer deposition (ALD) has surfaced recently as a solid-state electrolyte deposition method, since it offers uniform and conformal coating with controlled thickness. On the other hand, lithium metal is an ideal anode material, having a very high theoretical capacity of 3861 mAh/g. However, lithium is extremely reactive to the major gaseous components in the air and instantly forms a resistive passivation layer on the surface. This results in lithium plating with dendritic or mossy morphology, which may cause a short circuit. One of the major approaches to address these issues is forming an 'artificial' surface protection layer on the lithium metal, which is conductive to Li-ion transport but insulating for electronic conduction, protecting the lithium from unwanted electrochemical and chemical reactions.

We began by repeating previous research. We deposited a ZrO_2 metal oxide layer on a lithium disc using a dual plasma/thermal ALD process. Then, we successfully deposited a lithium-tantalum oxide solid-state electrolyte on a ZrO_2-coated lithium disc. We demonstrated that the ALD process can be used to deposit solid-state electrolytes on lithium discs. To perform the ALD deposition, we used two metal oxide subcycles—a Li_2O subcycle and a Ta_2O_5 subcycle—to deposit solid-state electrolytes. We used one subcycle of Li_2O with six subcycles of Ta_2O_5 ($1 \times Li_2O + 6 \times Ta_2O_5$ in brief) in a pulsing sequence to deposit lithium tantalum oxide solid-state electrolytes. Ta_2O_5 subcycles can be used in varying numbers to control the overall composition of the lithium tantalum oxide film ($Li_xTa_yO_z$). This approach can also be used to increase stability and tune the Li+ conductivity of the solid-state electrolyte film.

3. METHODS, ASSUMPTIONS AND PROCEDURES

3.1. Restarting the Process of Solid-State Electrolyte Deposition on Lithium Metal Using the PEALD Method

A Gemstar XT-DP Dual Manifold Thermal/PEALD Benchtop System, integrated with a dual glovebox, was used for solid-state electrolyte deposition. Last year's Covid pandemic interrupted this research, and the restarting process was slow. Late last year, we began to restart the PEALD system in the lab: we ordered Ar tanks, did basic maintenance work on the glovebox, updated the operating software for the PEALD system, and refilled and reorganized the precursors used in this project.

There were also several technical issues with the PEALD system that needed to be addressed in order to continue the project, including over-cooling of the manifold and signal instability of the RF generator for plasma. After these issues were addressed, we began reproducing phases of the results from our previous research. Reproducing our previous research served to test the restarted equipment. Also, since the continuous solid-state electrolyte deposition development builds on previous ZrO_2 metal oxide deposition, it was important and necessary to repeat our previous results.

3.1.1. ZrO_2 Metal Oxide Layer Deposition on Lithium Metal

The two kinds of substrate used in the ZrO_2 deposition were silicon wafer and Li-metal. The silicon wafer was cut into squares roughly 2 cm x 2 cm in size. Lithium discs (15.6 mm x 0.6 mm dia.) were purchased from MSE Supplies. The procedures of plasma/thermal dual ALD of ZrO_2 metal oxide were applied using the same methods as in our previous report.[4] Briefly, Tetrakis(dimethylamino)zirconium (TDMAZ, $C_8H_{24}N_4Zr$) was used as the zirconium precursor and was kept at 78 ℃ during the deposition process. Water was used as the oxidation precursor. A chamber temperature of 145 ℃ was kept constant during deposition process. The plasma/thermal dual procedures of ALD for ZrO_2 metal oxide deposition are shown in Figure 1.

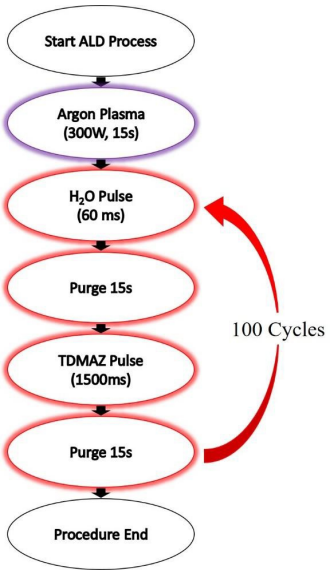

Figure 1. The Plasma/Thermal Dual ALD Process Flow for ZrO_2 Metal Oxide Deposition

3.1.2. Characterization of the PEALD ZrO_2 Layer

SEM images of a lithium disc coated with ZrO_2 (Figure 2A) and a pure lithium disc (Figure 2B) are shown in Figure 2. In comparison with a pure lithium disc (Figure 2B), the surface of the ZrO_2-coated lithium disc became rougher and granular in appearance (Figure 2A). Imaging shows that the deposited layer seems to be uniform and pin-hole free. To obtain a direct view of the ZrO_2 layer on the lithium surface, we made a cross-section of the disc. By tilting this cross-sectioned sample, the ZrO_2 layer can be observed more directly (Figure 2C). Because of conductivity difference, there is a clear contrast between the lithium and ZrO_2 layers. The granular appearance visible in Figure 2A can also be seen on the ZrO_2 layer shown in Figure 2C. Thus, the SEM images show the successful deposition of a uniform ZrO_2 metal oxide layer on the surface of the lithium disc.

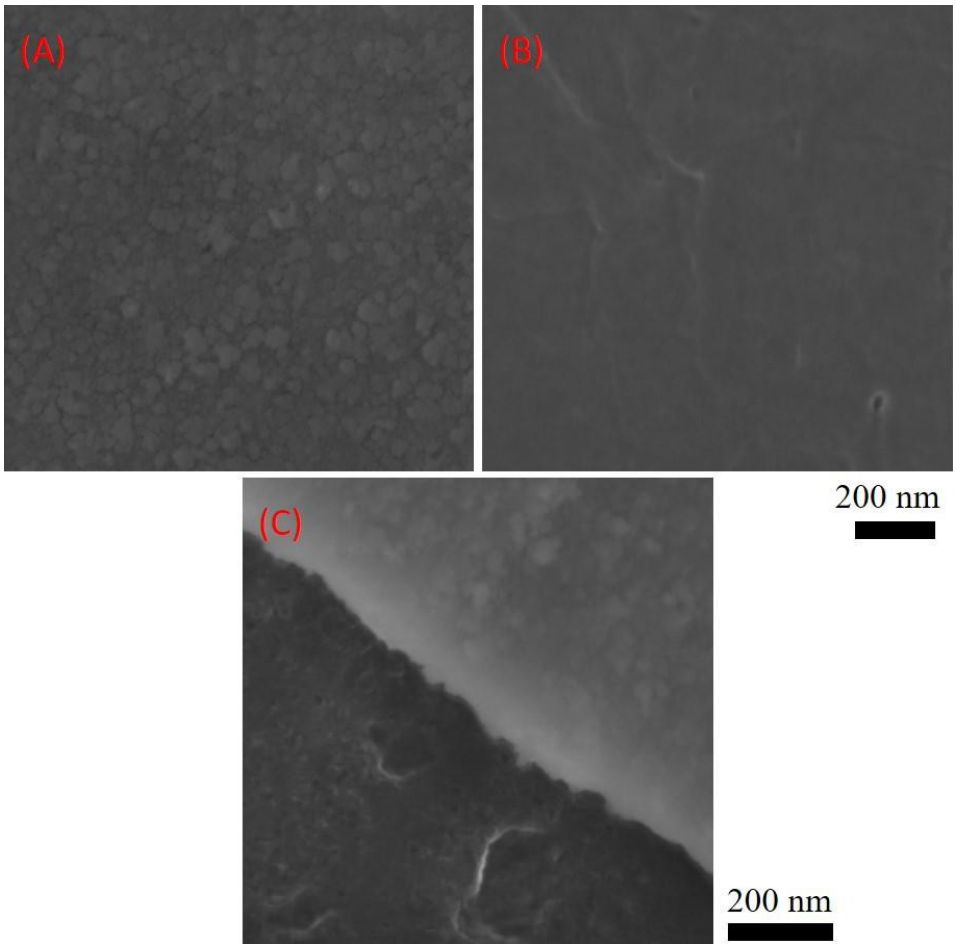

Figure 2. SEM Images of (A) Lithium Disc with ZrO_2 Metal Oxide Coating; (B) Pure Lithium Disc; and (C) Cross-section of a Cut Lithium Disc Coated with ZrO_2

To confirm the composition of the ALD-deposited layer, we used X-ray photoelectron spectroscopy (XPS) to identify the bonding condition of the deposited film. For the XPS measurement, a silicon wafer (silicon oxide on the surface of the silicon wafer) was used as a substrate for the plasma/thermal dual ALD deposition. To prevent lithium contamination of the XPS equipment, we did not use a lithium disc as a substrate for XPS measurement. A Thermo Scientific ESCALAB Xi+ X-ray Photoelectron Spectrometer Microprobe was used for this

measurement. The XPS survey scan (in Figure 3A) shows a 200 eV energy threshold with peaks identified. The rest of the peaks on Figure 3A are all zirconium peaks from different orbitals.

From the survey scan, there is no evidence of other elements in the film besides C, O, Zr, and Si. Figure 3B shows the Zr3d5/2 peaks for the deposited ZrO_2 layer on the silicon wafer. We used 20 eV as the pass energy level for the elemental fine scans. The adventitious carbon peak (284.8 eV) was used as a reference point, shifting all other peaks accordingly. Figure 3B shows that the Zr3d5/2 level peaks at 182.6 eV and 185.0 eV, respectively, matching with the peak positions of ZrO_2.[11] Therefore, the XPS measurement confirms that the plasma/thermal dual ALD method successfully deposited a ZrO_2 metal oxide layer.

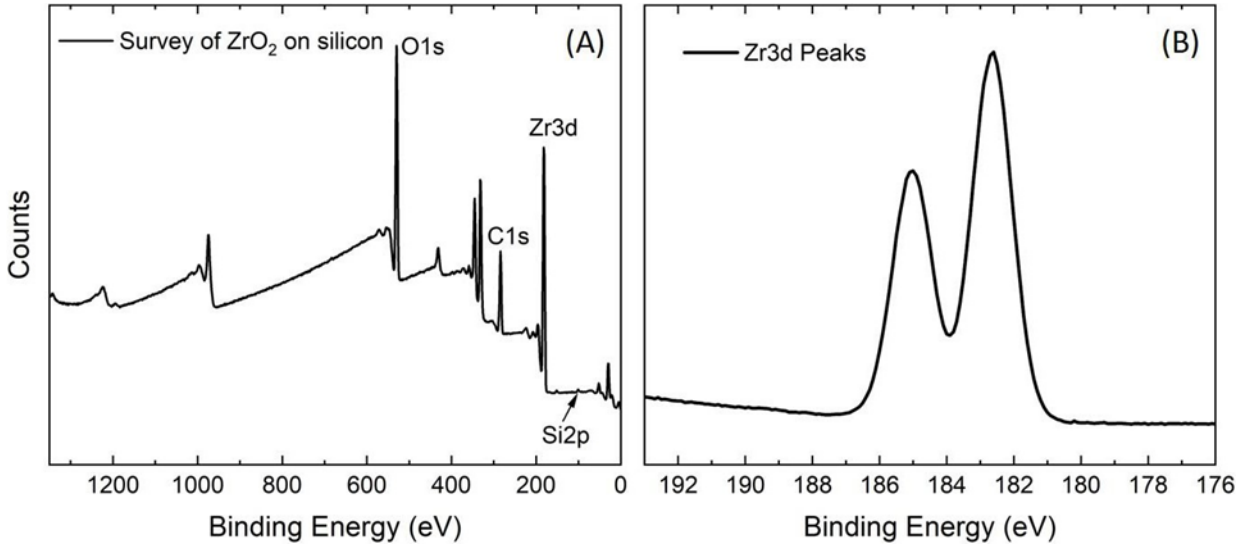

Figure 3. (A) XPS Survey Scan of ZrO_2 Deposited on Silicon Substrate and (B) Fine Scan of Zirconium $3d_{5/2}$ Peak Positions for Deposited ZrO_2 Layer

An MFP-3D Origin+ AFM from OXFORD Instruments was used to characterize the height profile of the deposited ZrO_2 layer, using a silicon wafer as the deposition substrate. There are several reasons why a lithium disc was not used for the AFM measurement. The primary reason is that lithium oxidizes in air, which can prevent accurate measurements. Also, lithium metal is soft while the lithium disc surface is very rough; these features are obstacles to accuracy. By contrast, a silicon wafer can achieve atomic flatness, which is ideal for height measurement of the deposited layer. Before ALD deposition, Kapton tape was used to partially mask the silicon wafer to prevent deposition of ZrO_2 on the substrate. The Kapton tape was removed after the ALD process, and its residue was removed with acetone. In this manner, a clear step profile of the ZrO_2 layer was created on the silicon substrate. Because surface conditions are crucial for ALD processes, a deposited layer using two different surfaces (lithium disc and silicon wafer) may have slight differences. However, the measured thickness of the silicon wafer still provided a fair estimate of the lithium disc thickness. Figure 4 shows AFM measurement of the ZrO_2 layer after 100 cycles of the ALD process. Five lines were used to calculate the height profile of the ZrO_2 layer (Figure 4A). The resulting height profiles of the five lines are shown in Figure 4B. This method shows that the thickness of the ZrO_2 layer measures between 36 nm and 40 nm. Therefore, the growth rate of a ZrO_2 metal oxide layer by the ALD process is between 3.6 Å and 4.0 Å per cycle.

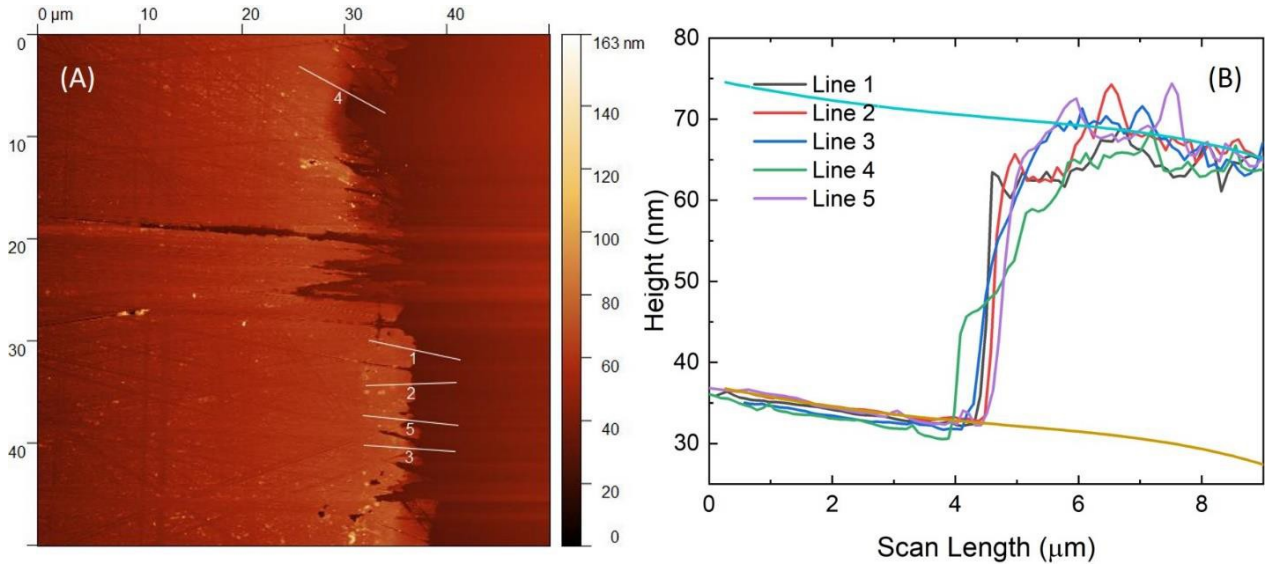

Figure 4. (A) AFM Height Image Near Step of ZrO_2 Layer; (B) Height Profile of 5 Lines Selected in (A)

3.2. Electrochemical Measurement of a Half-Cell Lithium Battery with an Optical Cell

3.2.1. Design of an Optical Cell for Electrochemical Measurement

Referencing our previous research, we repeated the electrochemical measurement of a half-cell lithium battery with a homemade optical cell.[4] The optical cell design is based on our previous research with the addition of small adjustments.[4] Briefly, 3 sheets of acrylic were used to make the 'sandwich; structure of the cell (Figure 5). The acrylic sheets measured 60 mm x 45 mm x 6.5 mm each. The left figure in Figure 5 shows the top view of the middle sheet of the optical cell. A rectangular hole measuring 11 mm x 24 mm was cut out of the middle of the sheet. Two nickel tabs of appropriate size were sandwiched between the middle and bottom sheets with epoxy, fixing their positions (right figure in Figure 5). By doing this, a "dent" was created on the bottom of the optical cell: the electrochemical characterization happens within this "dent". A homemade silicone rubber ring was used to seal the optical cell from the ambient environment for obtaining an electrochemical measurement. Smooth-On Mold Star 15 Platinum Silicone Rubber was used to make a rubber ring of appropriate size. Four metal clamps were used to apply force to the top and bottom of the panel sheets, sealing the optical cell to protect it from the ambient environment. The optical cell was assembled in an argon-filled glovebox. In this way, the optical cell protected the lithium metal from being oxidized, even though the electrochemical characterization happened outside the glovebox.

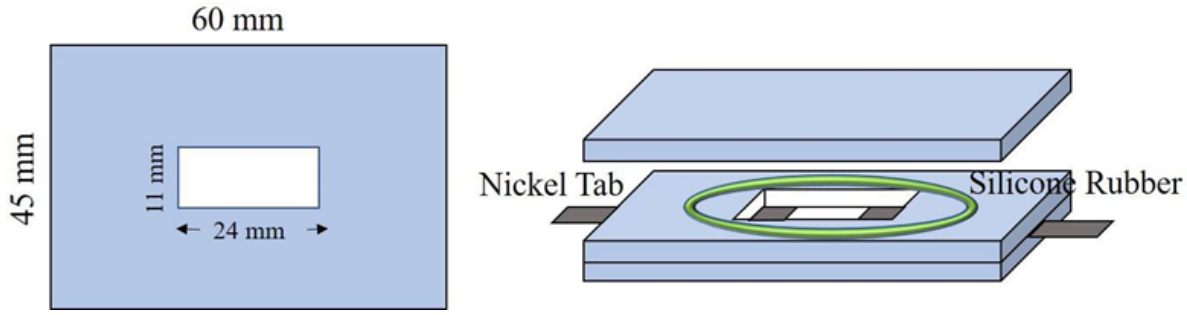

Figure 5. Design of the Optical Cell

3.2.2. Chronopotentiometry (CP) Measurement of a Symmetric Half-Cell

Both pure lithium discs and ZrO_2-coated lithium discs were used in this optical cell process for electrochemical measurement of a half-cell. A lithium disc was cut into a 10 mm x 10 mm square in order to fit into the optical cell. 100 cycles of ZrO_2 were deposited on each side of the square lithium disc. One lithium square (or ZrO_2-coated lithium square) was placed on each nickel tab. A carbon tap was used to connect the lithium disc (or ZrO_2-coated lithium disc) with the nickel tab in the optical cell. Two electrodes were separated inside the optical cell by a distance of roughly 5 mm. Measurement signals were collected through nickel tabs. A solution of lithium hexafluorophosphate solution in ethylene carbonate/dimethyl carbonate (V/V = 50/50) was purchased from Sigma-Aldrich, Inc., and was used without further purification as an electrolyte in the optical cell. Approximately 0.3 mL of lithium hexafluorophosphate solution was added into the optical cell to connect the two electrodes and make a symmetric half-cell. The sealed optical cell was then removed from the glovebox for conducting electrochemical characterization.

A VMP3 from BioLogic Science Instruments was used to conduct CP measurement on the optical cell. In our previous research, a current density of 4 mA/cm2 was kept constant during CP measurement.[4] Electrode potential in the optical cell was studied at a 4 mA/cm2 current density, with Li stripping/platting, for 10 minutes each over 100 cycles. Figure 6 compares the potential change of ZrO_2-coated and uncoated working electrodes with cycle number and elapsed time. Figure 6 (black line) shows that, for pure lithium electrodes, the initial potential needed to maintain the current is quite low (around 7.5 V), indicating that the impedance of a lithium electrode is quite small. However, over increasing cycle numbers, the potential needed to maintain the current increases steadily, reaching around 11 V at the end of the measurement phase. This proves that the impedance of a lithium electrode increases along with the cycle number. On the other hand, the potential of lithium electrodes with a ZrO_2 coating is initially larger than the potential of pure lithium electrodes (Figure 6, red line). However, the amplitude of potential remains steady throughout all cycles. Therefore, the potential of lithium electrodes with a ZrO_2 coating is lower than that of pure lithium electrodes. These results indicate that the initial impedance of ZrO_2-coated lithium is greater than that of pure lithium. However, the deposited ZrO_2 layer inhibits the increase of impedance in lithium electrodes throughout cycles. Hence, the deposited ZrO_2 layer increases the stability of the lithium electrode. Similar results were observed in our previous research.[4]

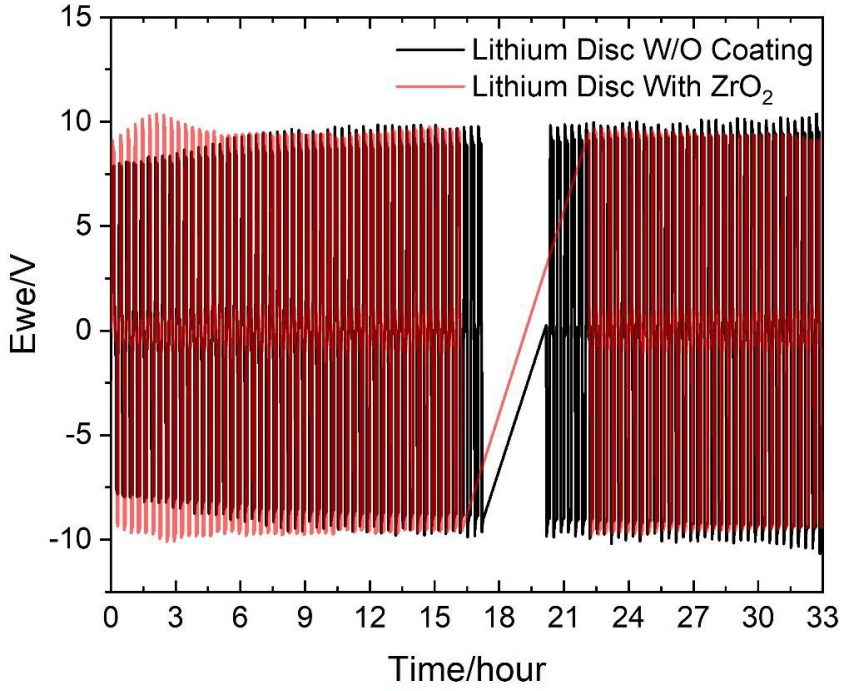

Figure 6. Potential Change in Working Electrodes over Time under Constant Current Density for Lithium Discs with and without ZrO_2 Coating

The suppression of increased impedance when using a deposited ZrO_2 layer can be explained by the prevention of dendrite formation. Figure 7 shows an optical cell after 100 cycles CP measurement. Dendrite formation can be observed in the pure lithium electrode (Figure 7A). However, there is no obvious dendrite formation in the lithium electrode with a ZrO_2 coating (Figure 7B). These observations further confirm that the deposited ZrO_2 layer on lithium suppresses lithium dendrite formation along the solid-liquid interface of the lithium-ion battery, while increasing stability of the lithium anode. At this point, we successfully repeated what was achieved in our earlier research. Building on these achievements, we could further investigate the deposition of lithium-tantalum oxide solid-state electrolytes on a lithium disc.

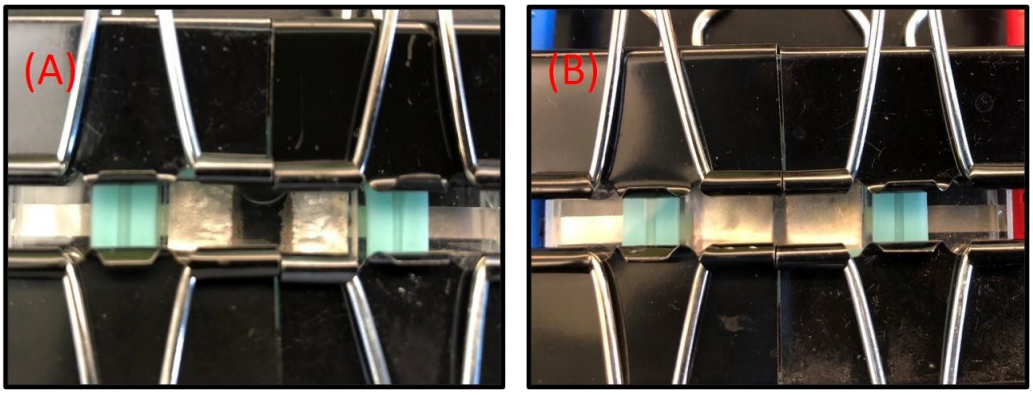

Figure 7. Optical Images of a Lithium Disc without Coating (A) and a Lithium Disc with a ZrO_2 Coating (B) in an Optical Cell after 100 Cycles of CP Measurement

3.3. Lithium Tantalum Oxide Solid-State Electrolyte Deposition Using PEALD

After deposition of a ZrO_2 metal oxide layer on a lithium disc to increase its thermal and electrochemical stability, our next step was to deposit lithium-tantalum oxide solid-state electrolytes on top. Lithium tantalum oxide was chosen as the solid-state electrolyte for the lithium-ion battery because it fits several criteria. First of all, it is lithium-ion conductive, even for amorphous structures. Previous studies showed that lithium tantalum oxide in amorphous structures is lithium-ion conductive, as opposed to crystalline structures, which were not conductive.[5,6] This is advantageous in the ALD process because is the formation of amorphous lithium tantalum oxide is expected during the process. Thus, the deposited solid-state electrolyte can be used directly after the ALD process without further annealing at high temperature, which can be time consuming and can introduce defects in the film. Second, the lithium-ion conductivity of lithium tantalum oxide makes it acceptable for use as a solid-state electrolyte (10- 5--10-8 S/cm). Third, lithium tantalum oxide is insulated for electronic conductivity at room temperature.[5,6] This prevents side reactions and battery energy leakage. Therefore, we chose to focus our research on the deposition of lithium tantalum oxide on lithium discs to be used as a solid-state electrolyte.

Some research articles reported the successful deposition of solid-state electrolyte on a silicon wafer.[4,7-9] However, there are few reported successes for similar deposition on lithium metal. This is because the deposition temperature necessary for ALD is relatively high (above 200 ℃, sometimes even above 300 ℃). As we know, the melting temperature of lithium is around 170 ℃ to 180 ℃. Thus, a high deposition temperature prevents these materials from being applied to lithium discs directly. This brings up the importance of the deposition of a ZrO_2 layer on lithium discs, which has proven to increase the discs' thermal stability. This is also one of the reasons we choose ZrO_2 as the protective layer to be deposited on the lithium surface. With a layer of ZrO_2 metal oxide on a lithium disc, we can reasonably increase the temperature of the ALD process in order to achieve the deposition of solid-state electrolytes. Argon plasma was used to further lower the energy barrier of the reaction, and to reduce the deposition temperature.

Lithium tert-butoxide (LiOtBu, (CH3)3COLi) and tantalum(V) ethoxide (TaEO, (CH3CH2O)5Ta) were purchased from STREM Chemicals to be used as sources of lithium and tantalum, respectively. Water was used as an oxidant. Silicon wafer and ZrO_2-coated lithium discs were used as substrates for the deposition. A Gemstar XT-DP Dual Manifold Thermal/PEALD Benchtop System integrated with a dual glovebox was used for this deposition.

3.4. Use of the PEALD Procedure for Lithium Tantalum Oxide Solid-State Electrolyte Deposition

The PEALD procedure for lithium tantalum oxide deposition was adopted from our previous study, with some adjustments.[4] The deposition of lithium tantalum oxide was conducted at a temperature of 175 ℃. The process consisted of two subcycles: lithium oxide (Li_2O) and tantalum oxide (Ta_2O_5). Figure 8 shows the PEALD process flow for the solid-state electrolyte deposition. The Li_2O subcycle consisted of a water pulse (120 ms) alternated with a LiOtBu pulse (2000 ms), while the Ta_2O_5 subcycle consisted of a water pulse (120 ms) alternated with a TaEO pulse (30 ms to 600 ms). Both the LiOtBu and TaEO sources were heated to 175 ℃ during the deposition. A pulse time of 30 ms to 600 ms was used for the TaEO source. Between each pulse, there was a purge of 10 or 15 seconds to remove any excess of precursor from the chamber. As shown in Figure 8, for each Li_2O subcycle, there are four or six Ta_2O_5 subcycles.

This can be expressed as 1 × Li_2O + 6 × Ta_2O_5. Both silicon wafers and ZrO_2-coated lithium discs were used as substrates during the lithium tantalum oxide solid-state electrolyte deposition process.

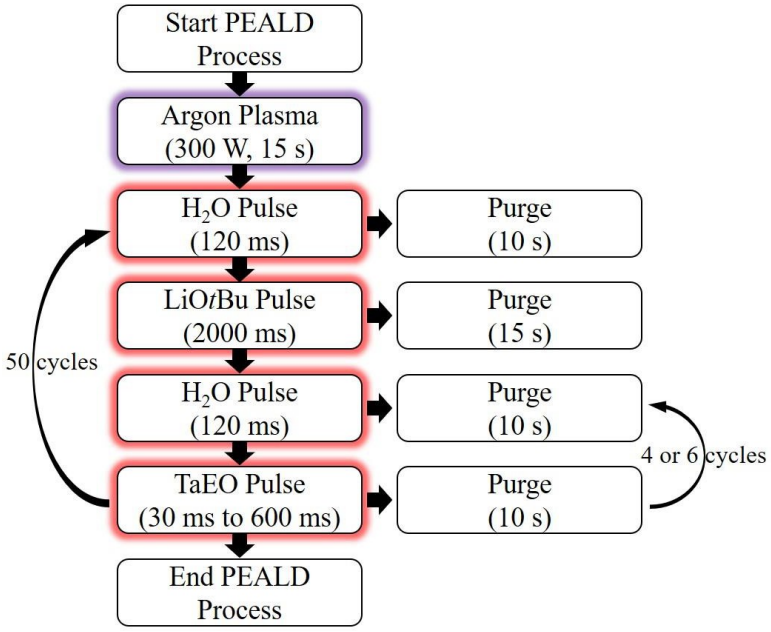

Figure 8. The PEALD Process Flow for Lithium Tantalum Oxide Deposition

3.5. Characterization of Deposited Lithium Tantalum Oxide Solid-State Electrolyte

3.5.1. SEM Imaging and Elemental Mapping of Deposited Lithium Tantalum Oxide Solid-State Electrolytes

Because our Zeiss Auriga FIBFESEM is currently under repair, we could not perform SEM imaging, EDS, or elemental mapping of the deposited lithium tantalum oxide solid-state electrolyte. Had the SEM still been down upon the writing of this report, we would have included an attachment containing the SEM images and elemental mapping data of the solid-state electrolyte. The other characterization results given here provide information similar to those obtained from SEM elemental mapping.

3.5.2. XPS Measurement of Lithium Tantalum Oxide Solid-State Electrolytes

As illustrated in Figure 8, we used 30 ms and 600 ms pulses of TaEO in the deposition of lithium tantalum oxide layers. To prevent lithium contamination of the equipment, the XPS measurement was taken from lithium tantalum oxide film deposited on a silicon wafer substrate. Composition of the lithium tantalum oxide film ($Li_xTa_yO_z$) can be measured from survey scans of the solid-state electrolyte film (Figure 9A). By integrating the area under each peak, the atomic ratio between elements can be calculated. During the 30 ms TaEO pulse, the Li and Ta ratio was 21:9 ($Li_21.9TaO_z$), while the ratio fell to 12:6 during the 600 ms TaEO pulse (Li12.6TaOz). The elemental composition of lithium tantalum oxide film calculated from the survey scan is shown in Table 1. Data in the table shows that a longer pulse time increases the tantalum content. However, the increase in metal oxide is not proportional to the increase in pulse duration. (A 20x increase in TaEO pulse duration does not result in a 20x increase in metal oxide.) This observation makes sense because the ALD process is self-limiting in nature. When the reactive

species on the surface have fully reacted, adding more reactant does not increase the overall reaction. Accordingly, a longer pulse of reactant does not deposit a correspondingly increased amount of metal oxide.

Table 1. Elemental Composition of a Lithium Tantalum Oxide Layer Deposited with Different Pulse Durations Using a Pulsing Sequence of 1 × Li_2O + 6 × Ta_2O_5 as Measured by XPS Survey Scans

TaEO pulse duration (ms)	Ta (at%)	Li (at%)	C (at%)	O (at%)	Chemical formula
30	0.56	12.28	32.49	54.67	$Li_{21.9}TaO_z$
600	0.64	8.05	28.1	63.2	$Li_{12.6}TaO_z$

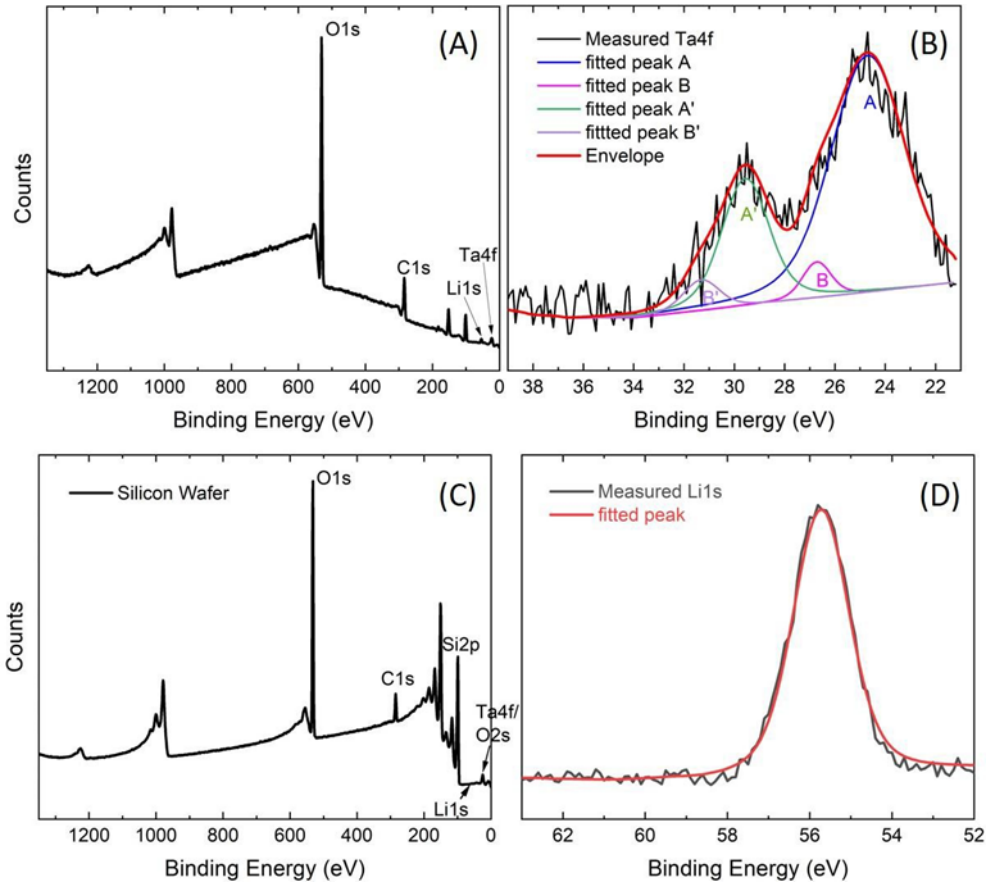

SFigure 9. An XPS Survey scan of Lithium Tantalum Oxide Film (A) and Silicon Wafer (C); (B) a Tantalum 4f Fine Scan with 2 Sets of Peak Deconvolution, A, B & A', B'(A: 24.7 eV, B: 26.7 eV, C: 29.5 eV, D: 31.3 eV binding energy); and (D) a Lithium 1s Fine Scan with Fitted Peak at 55.7 eV Binding Energy

Figure 9B and Figure 9D illustrate the elemental fine scans of the tantalum 4f and lithium 1s peaks, respectively. The existence of tantalum and lithium peaks proves that the ALD deposition of lithium tantalum oxide film was successful. Comparing Figure 9A and Figure 9C, we can see that there is no Li1s peak for the silicon wafer, while there is an Li1s peak for the lithium tantalum oxide film. Obviously, Si2p peaks are more predominant for silicon wafers than for lithium tantalum oxide film. We deconvoluted the measured tantalum 4f peak into two sets of peaks: A, B & A', and B' (Figure 9B). The binding energy levels for A and B are 24.7 eV and 26.7 eV respectively, corresponding with the Li-O-Ta binding in the lithium tantalum oxide film. Conversely, the higher binding energy levels of A' and B' (29.5 eV and 31.3 eV) are similar to tantalum oxide (Ta_2O_5) binding. Therefore, the A' and B' peaks are corresponding with Ta-O-Ta

binding in the lithium tantalum oxide film. This peak deconvolution indicates that the tantalum element within the lithium tantalum oxide film has two types of chemical environments: Li-O-Ta and Ta-O-Ta binding. From the deconvolution results, the ratios of Ta in Li-O-Ta and Ta-O-Ta are 71.2% and 28.8%, respectively. The Ta-O-Ta binding element results from multiple Ta_2O_5 subcycles during the ALD deposition process. Figure 9C shows the Li1s peak (55.7 eV), which is a level of lithium binding energy indicating lithium oxide, as expected. The XPS measurements indicate successful deposition of lithium tantalum oxide film from the ALD process. The XPS measurements also indicate that there are two types of Ta chemical environments—Li-O-Ta and Ta-O-Ta—present within the film.

The carbon 1s peak for different TaEO pulse durations was also measured for the lithium-tantalum oxide film (Figure 10), yielding some interesting results. Figure 10A shows the carbon 1s peak of deposited film after a 30 ms TaEO pulse duration. A lower binding energy level of 284.8 eV corresponds to the adventitious carbon (C-C), while the higher binding energy level of 290.0 eV is the carbonate peak (CO32-). The carbonate found in the XPS measurement is the result of a reaction between Li_2O and CO_2 when lithium oxide is exposed to air.[8] This carbonate has also been found in other lithium-containing films deposited by the ALD process.[10] By peak deconvolution, Figure 10A indicates that the carbonate content is quite high (42.8%). However, the deposition results after a 600 ms TaEO pulse duration (Figure 10B) show that carbonate content is significantly reduced (10.5%). This result shows that a Ta_2O_5 subcycle can effectively prevent a lithium element side reaction during air exposure by forming more Ta-O-Ta binding type in the film. Consequently, we can further stabilize lithium tantalum oxide film by using more than six Ta_2O_5 subcycles. However, according to previous research, there is a consequence: more Ta_2O_5 binding type within the lithium tantalum film decreases both the lithium content and the lithium-ion conductivity.[4] In order for the solid-state electrolyte to operate efficiently, sufficient lithium-ion conductivity is necessary. Additional research is needed in order to optimize these parameters for application.

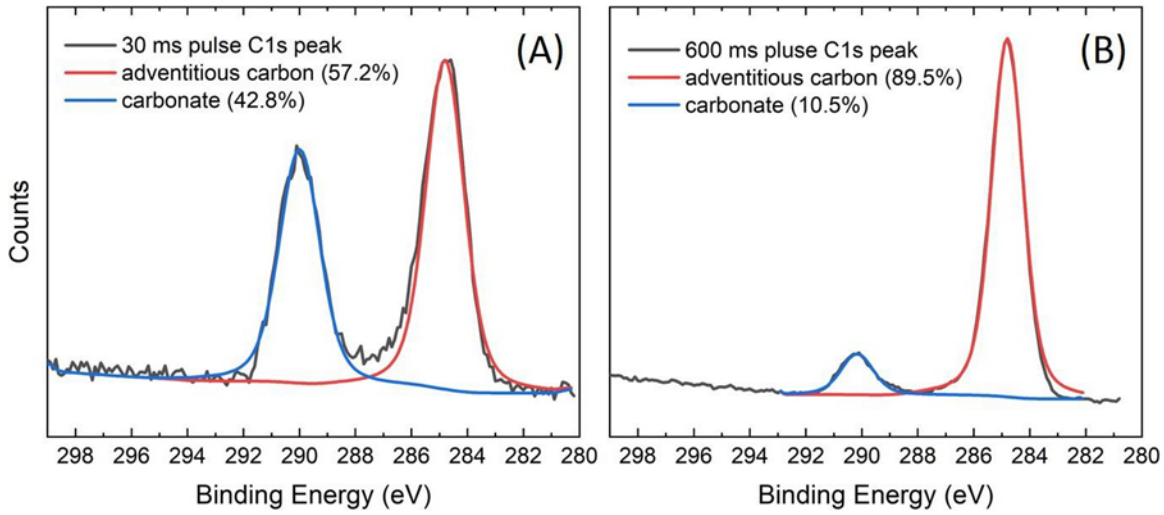

Figure 10. An XPS Carbon 1s fine scan and corresponding peak deconvolution of lithium tantalumoxide film with a 30 ms TaEO pulse duration (A) and a 600 ms TaEO pulse duration (B).

3.5.3. AFM Scan and Deposition Rate of a Lithium Tantalum Oxide Layer Deposited Using theALD Process

The thickness of lithium tantalum oxide layers was measured with an MFP-3D Origin+ AFM from OXFORD Instruments (Figure 11). The step between the ZrO_2 and lithium tantalum oxide layers was created with a mask during the ALD deposition process. Kapton tape was used to block certain parts of the substrate after the initial deposition of the ZrO_2 layer. Another step was created after the Kapton tape was removed following the deposition of lithium tantalum oxide layer. For the purposes of AFM measurement, only silicon wafers were used as the deposition substrate. Air sensitivity of lithium discs invalidated them from being used as a substrate for AFM measurements, which is the same for the thickness measurement of ZrO_2 layer. Figure 11A shows the 20 µm × 20 µm area scan of the lithium tantalum oxide step region. Six lines were selected within this area to measure the thickness of the deposited layer. The six step profiles are shown in Figure 11B. Using the individual thickness measurements of the six lines, the average thickness of the deposited lithium tantalum oxide layer was calculated as 31.4 ± 1.1 nm.

Therefore, the deposition rate of a lithium tantalum oxide layer is about 6.3 Å per cycle, using an ALD recipe of 1 × Li_2O + 6 × Ta_2O_5.

The roughness of the deposited lithium tantalum oxide layer was also studied with a larger scan area. Figure 12 shows a 50 µm × 50 µm AFM scan of a lithium tantalum oxide layer on a silicon substrate. From this scan, the mean roughness (Sa) was measured at 3.13 nm, and the root mean square (RMS) roughness (Sq) was measured at 4.1 nm. These roughness measurements show that the ALD deposited solid-state electrolyte is evenly smooth and uniform, with a metal oxide deposition (40 nm ZrO_2 layer and 30 nm lithium tantalum oxide layer) at a thickness of about 70 nm. The ALD method is capable of depositing a uniform metal oxide layer while maintaining excellent thickness uniformity of the deposited layer. While good for the deposition of thin film, the ALD method can also produce uniform, controlled deposits on complicated 3D structural substrates. Therefore, the ALD method can be used successfully for deposition on electrodes with 3D architecture to further increase battery performance.

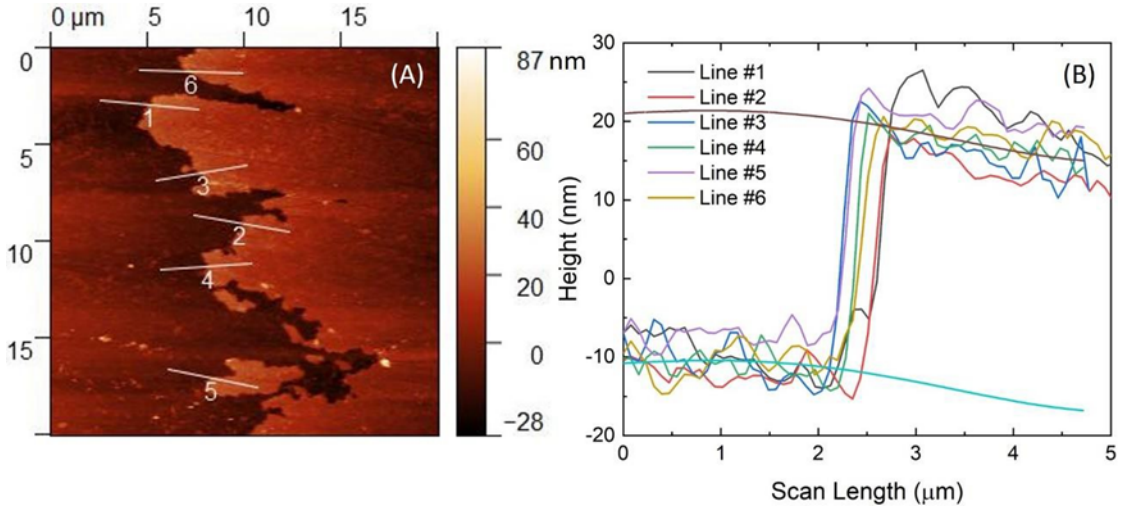

Figure 11. A 20 µm × 20 µm AFM scan (A) of the step height profile of ZrO_2 and lithium tantalum oxide layers (six lines were selected within to study the thickness of the depositedlithium tantalum oxide layer); a (B) step profile of six lines selected in (A).

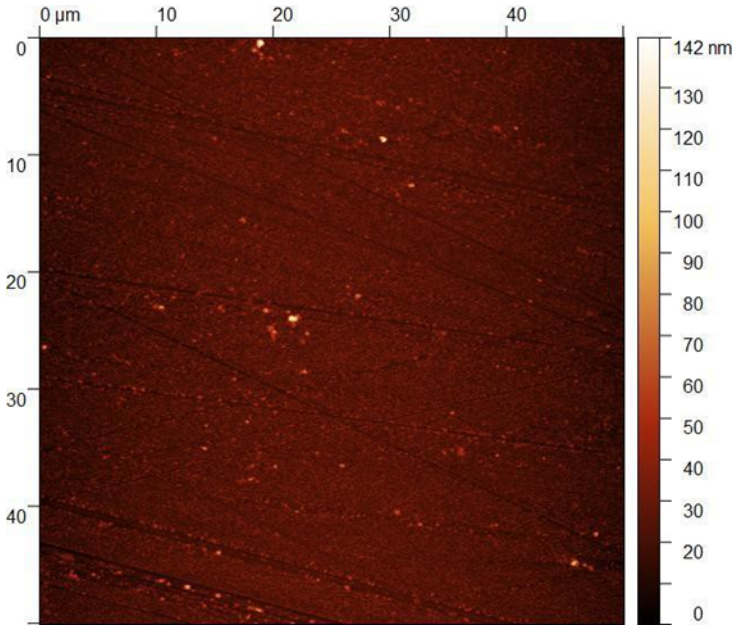

Figure 12. AFM Scan of 50 µm × 50 µm Area of Deposited Lithium Tantalum Oxide Layer on Silicon Substrate

3.5.4. Resistivity Measurement of Lithium Tantalum Oxide Film by Four Point Probe

A Jandel Four Point Probe was used to measure the resistivity level of deposited lithium tantalum oxide film. For this measurement, a silicon wafer was used as a substrate to initially deposit 100 cycles of a ZrO_2 layer, followed by 50 cycles of lithium tantalum oxide on top. The four probes penetrate the deposited layer outside, contacting the lithium metal directly, providing a measurement of the lithium metal, rather than the deposited lithium tantalum oxide layer. A lithium disc substrate was also measured, but was too soft after being coated. Silicon wafers, on the other hand, are very hard and can withstand the pressure of the probes. An 80 µA current was used, producing a measured resistivity level of 2.0 kΩ per square for lithium tantalum oxide film. This result shows that the deposited solid-state electrolyte has sufficient resistivity to prevent energy leakage and side reactions during the charging and discharging cycles of lithium-ion batteries.

4. RESULTS AND DISCUSSION

We began by restarting the glovebox, fixing or replacing parts of the PEALD system, and making necessary system updates. We then attempted to repeat our previous research results. We deposited a ZrO_2 metal oxide layer on a lithium disc using a dual thermal/plasma ALD process. Then, we confirmed the morphology of the deposited ZrO_2 layer through SEM imaging. XPS confirmed the binding conditions for ZrO_2. A deposition rate of 4 Å per cycle was calculated using AFM measurement. We also demonstrated, using a homemade optical cell, that a layer of ZrO_2 deposited on a lithium disc can indeed prevent dendrite formation during the charge and discharge cycles of a lithium battery. In summary, we successfully repeated all the achievements from our previous research.

The second part of this study focused on the deposition of lithium tantalum oxide solid-state electrolyte layer on top of a ZrO_2-coated lithium disc using the ALD process. The deposition temperature was reduced from 225 ℃ to 175 ℃. We used a similar recipe for ALD deposition of lithium tantalum oxide on a silicon substrate.[4] A pulsing sequence of $1 \times Li_2O + 6 \times Ta_2O_5$ was used for the deposition, resulting in a deposition rate of 6.3 Å per cycle. XPS measurements indicated that the deposition of a lithium tantalum oxide layer using the ALD process was successful. XPS measurements also indicated that there are two types of chemical binding within the lithium tantalum film: Li-O-Ta and Ta-O-Ta. The ratio of the two binding types is closely related to the TaEO pulse duration and the number of Ta_2O_5 subcycles. The composition of lithium tantalum oxide film ($Li_xTa_yO_z$) can also be tuned by the number of Ta_2O_5 subcycles. We also found that Ta_2O_5 can prevent the lithium element on the surface of a lithium tantalum oxide layer from reacting with CO_2 in air. Therefore, it can be used to increase the stability of lithium tantalum oxide film. However, too much Ta in the lithium tantalum oxide film will reduce the Li+ conductivity of the deposited layer, which is detrimental to the usage of solid-state electrolytes in batteries. The resistivity of lithium tantalum film is 2.0 kΩ per square; as a solid-state electrolyte, this is sufficient to prevent energy leakage and side reactions in batteries.

5. CONCLUSION

For future studies, a prototype of a lithium battery with a solid-state electrolyte could be used to test the performance of various solid-state electrolytes. Based on this prototype, multiple parameters of the ALD process could be tested to determine the optimal deposition conditions, such as the thickness of the solid-state electrolyte layer, deposition temperature, the number of subcycles used, and so on. Anodes with complicated 3D architectures could also be used to deposit solid-state electrolytes and then tested for performance.

REFERENCES

[1] Long, J. W.; Dunn, B.; Rolison, D. R.; White, H. S. Three- Dimensional BatteryArchitectures. Chem. Rev. 2004, 104, 4463−2292.

[2] Roberts, M.; Johns, P.; Owen, J.; Brandell, D.; Edstrom, K.; Enany, G. E.; Guery, C.; Golodnitsky, D.; Lacey, M.; Lecoeur, C.; et al. 3D Lithium Ion Batteries−from Fundamentals to Fabrication. J. Mater. Chem. 2011, 21, 9876−9890.

[3] Oudenhoven, J. F. M.; Baggetto, L.; Notten, P. H. L. All-Solid- State Lithium-Ion Microbatteries: a Review of Various Three- Dimensional Concepts. Adv. Energy Mater.2011, 1, 10−33.

[4] Pankaj Kumar Alaboina, Stanley Rodrigues, Michael Rottmayer, Sung-Jin Cho*, "In-Situ Dendrite Suppression Study of Nanolayer Encapsulated Li Metal Enabled by Zirconia Dual Atomic Layer Deposition." ACS Applied Materials & Interfaces. Aug 2018

[5] Glass, A. M.; Nassau, K.; Negran, T. J. Ionic Conductivity of Quenched Alkali Niobateand Tantalate Glasses. J. Appl. Phys. 1978, 49, 4808−4811.

[6] Li, Z.; Chen, X.; Hu, X. The Preparation of Ionic Conductance of Nano-AmorphousLi_XTaO_Y Thin Film. J. Phys. D: Appl. Phys. 1996, 29, 2740−2744.

[7] Putkonen, M.; Aaltonen, T.; Alnes, M.; Sajavaara, T.; Nilsen, O.; Fjellvag̊, H., AtomicLayer Deposition of Lithium Containing Thin Films. J. Mater. Chem. 2009, 19, 8767−8771.

[8] Aaltonen, T.; Alnes, M.; Nilsen, O.; Costelle, L.; Fjellvag̊, H. Lanthanum Titanate and Lithium Lanthanum Titanate Thin Films Grown by Atomic Layer Deposition. J. Mater.Chem. 2010, 20, 2877− 2881.

[9] Ham̈ al̈aïnen,J.;Munnik,F.;Hatanpaä,̈T.;Holopainen,J.; Ritala, M.; Leskela,̈M. Study of Amorphous Lithium Silicate Thin Films Grown by Atomic Layer Deposition. J. Vac. Sci. Technol., A 2012, 30, 01A106.

[10] Miikkulainen, V.; Nilsen, O.; Laitinen, M.; Sajavaara, T.; Fjellvag̊, H. Atomic Layer Deposition of $Li_XTi_YO_Z$ Thin Films. RSC Adv. 2013, 3, 7537−7542.

[11] Jerome, R.; Theyssie, Ph.; Pireaux, J.J.; and Verbist, J.J. Surface analysis of polymers end-capped with metal carboxylates using X-ray photoelectron spectroscopy. Appl. Surf.Sci. 1986, 27, 93.